

Novel Effect of Hyaluronan and Proteoglycan Link Protein 1 (HAPLN1) on Hair Follicle Cells Proliferation and Hair Growth

Hae Chan Ha^{1#}, Dan Zhou^{1,2#}, Zhicheng Fu^{1,2}, Moon Jung Back¹, Ji Min Jang^{1,2}, In Chul Shin^{1,2} and Dae Kyong Kim^{1,2*}

¹Department of Environmental & Health Chemistry, College of Pharmacy, Chung-Ang University, Seoul 06974, ²Hapln-Science Research Institute, HaplnScience Inc., Seongnam-Si 13494, Republic of Korea.

***Corresponding author:** Dae Kyong Kim. Daewangpangyo-Ro 660, Bundang-Gu, Seongnam-Si, Gyeonggi-Do CP: +82-10-6353-0938. Tel: +82-31-724-2611. Fax: +82-31-724-261. E-mail: kimdk@hapln-science.com

Tel: +82-31-724-2611, Fax: +82-31-724-2612

#: Hae Chan Ha and Dan Zhou have contributed equally to this work.

Running title: HAPLN1 Enhances Hair Follicle Growth
Number of words in the text from Abstract to Discussion: 4422

Number of figures: 6

Number of references: 34

Abstract word count: 218

Discussion word count: 850

Abstract

Hair loss is a common condition that can have a negative impact on an individual's quality of life. The severe side effects and the low efficacy of current hair loss medications create unmet needs in the field of hair loss treatment. Hyaluronan and Proteoglycan Link Protein 1 (HAPLN1), one of the components of the extracellular matrix, has been shown to play a role in maintaining its integrity. HAPLN1 was examined for its ability to impact hair growth with less side effects than existing hair loss treatments. HAPLN1 was predominantly expressed in the anagen phase in three stages of the hair growth cycle in mice and promotes the proliferation of human hair cells. Also, HAPLN1 was shown to selectively increase the levels of transforming growth factor- β receptor II in human hair cells. Furthermore, we observed concomitant activation of the ERK1/2 signaling pathway following treatment with HAPLN1. Our results indicate that HAPLN1 elicits its cell proliferation effect via the TGF- β 2-induced ERK1/2 pathway. The prompt entering of the hair follicles into the anagen was observed in the old mice group that received intraperitoneal injection of HAPLN1, compared to the vehicle-treated group. Insights into the mechanism underlying such hair growth effects of HAPLN1 will provide a novel potential strategy for treating hair loss with much lower side effects than the current treatments.

Keywords: HAPLN1, Hyaluronic Acid, CD44, TGF- β receptor II, ERK1/2, HHGMCs

Introduction

An estimated 147 million people suffer from hair loss worldwide, with an estimated 50% of men and women experiencing forms of pattern baldness at some point in their lives. Hair serves many features, providing insulation, protection, and a friction buffer; however, the aesthetic function of hair is arguably the most important for human beings because it is directly related to our sociality and self-esteem. Common treatments for hair loss include conventional chemical methods such as minoxidil, finasteride, herbal extracts, platelet-rich plasma (PRP), keratinocyte-conditioned media, adipose-derived stem cells, and hair transplantation. However, none of these methods are known to bring satisfactory results (Taghiabadi et al. 2020).

The hair follicle is an organ composed of inner and outer layers, bulge, bulb, and sebaceous glands (Hibino and Nishiyama 2004; Philpott et al. 1990). The hair follicles undergo a hair growth cycle. Through the growing (anagen), degenerating (catagen), and resting periods (telogen), the hair repeats growth and loss (Chase 1954). The anagen phase, the development process of dermal papilla (DP) and matrix cells, plays a crucial role in hair formation. Dermal papilla has blood vessels and nourishes matrix cells. In the matrix, hair is formed through the differentiation, proliferation, and keratinization of cells. The thickness and length of the hair are determined by the condition of dermal papilla and matrix cells. Several signaling molecules are involved in the normal hair follicle cycle, including Wnt, BMP, shh, and TGF- β signaling cascades (Niimori et al. 2012). TGF- β 1 is known to inhibit the proliferation of keratinocytes (Mori et al. 1996; Foitzik et al. 2000). In a previous study, the onset of catagen in TGF- β 1 $-/-$ mice was slower than in the control group. While an injection of TGF- β 1 into the dorsal skin of the mice induced catagen development (Foitzik et al. 2000). In contrast, TGF- β 2 signal plays an important role in hair follicle morphogenesis and hair follicle stem cell activation (Hibino and Nishiyama 2004; Oshimori and Fuchs 2012). This notion is further supported by animal studies in which Tgfb2-null skin exhibited a delay in hair follicle morphogenesis (Foitzik et al. 1999).

TGF- β signaling contains two pathways: Smad-dependent or non-Smad-dependent pathways. In the canonical TGF- β pathway, TGF- β ligands bind to the TGF- β receptor I (T β RII) homodimers on the membrane with high affinity. T β RII dimerizes with TGF- β receptor I (T β RI) homodimers and activates T β RI by T β RII-mediated phosphorylation. The T β RI-T β RII complex undergoes either clathrin-mediated (non-raft) or caveolae-mediated (lipid-raft) endocytic pathway, and each pathway is determined by membrane trafficking of the T β RI-T β RII complex. Internalization of the T β RI-T β RII complex through clathrin-mediated endocytosis activates Smad2/3 pathway, and the internalized receptors can be recycled and return to the membrane. In contrast, caveolae-mediated endocytosis induces degradation of T β RI-T β RII complex (Huang and Chen 2012). In the non-canonical pathway, TGF- β activates Smad-independent pathways such as PI3K/Akt, and MAPK pathway (Neuzillet et al. 2013; Derynck and Zhang 2003). MAPKs, comprising JNK, p38, and ERK, are considered to play crucial roles in hair follicle morphogenesis and regeneration (Tang et al. 2019).

In the present study, we focus on the roles of Hyaluronan and proteoglycan link protein-1 (HAPLN1) in the hair cycle. HAPLN1, previously referred to as a link protein, is a glycoprotein that is distributed in various tissue organs such as cartilage, skin, brain, heart, a

and kidney and stabilizes non-covalent interactions between aggrecan and hyaluronic acid (HA) in proteoglycans (PGs) aggregates (Binette et al. 1994; Spicer et al. 2003; Hardingham 1979). HA is a simple repeating disaccharide polymer, mainly found in the dermis and epidermis (50% of total body HA contents) (Papakonstantinou et al. 2012). One of the main characteristics of HA is its ability to hold water molecules, so it plays a vital role in keeping the skin hydrated and preventing the aging of skin and hair (Xi et al. 2021). As the ECM gradually degrades with age, HA also degrades along with it (Campiche et al. 2019). But HAPLN1 can retard the degradation of HA. A previous study has shown that HA levels were dramatically reduced in HAPLN1 knockdown, suggesting that loss of HAPLN1 protein affects the stability of HA (Govindan and Iovine 2014). In hair, some studies have shown that HA promoted hair growth by promoting follicle growth (Kim et al. 2022).

In our previous study, using surgically anastomosed parabiotic mice and the aptamer-based proteomic analysis of their blood proteins, we identified HAPLN1 as a protein associated with skin aging. We have evaluated whether age-related decreases in the levels of collagen and HA, major structural components of the ECM, can be restored by exposure to youthful circulation (Fu et al., submitted for publication).

In the present study, we investigated the anti-aging effects of HAPLN1 on hair follicles. We focused on the proliferation of human hair germinal matrix cells (HHGMCs) and the mechanism by which recombinant human HAPLN1 (rhHAPLN1) is involved in the *in vitro* cell proliferation and *in vivo* hair growth in old mice. Our results revealed that rhHAPLN1 enhanced TGF- β 2 signaling in a non-canonical pathway via the selective increase in TGF- β receptor II (T β RII) in HHGMCs and showed that intraperitoneal injections of rhHAPLN1 into the synchronized old mice increased the hair growth through the earlier entrance into the anagen phase of the hair follicles.

Materials and Methods

Chemicals and reagents

Recombinant human TGF- β 2 (302-B2-010/CF, R&D Systems, Minneapolis, MN, USA) was used as well as 4-methylumbelliferone (M1381, Sigma, St Louis, MO, USA), hyaluronic acid (73641, Sigma, St Louis, MO, USA) and recombinant human HAPLN1 (WUXI, Shanghai, China).

Cell and culture

Human hair germinal matrix cells (HHGMCs, 2410, ScienCell, Carlsbad, CA, USA) were purchased from ScienCell Research Laboratories (Carlsbad, CA) and maintained in mesenchymal stem cell medium (MSCM7510, ScienCell, Carlsbad, CA, USA) and 5 ml FBS, 1% mesenchymal stem cell growth supplement (MSCGS, 7552, ScienCell, Carlsbad, CA, USA), and 1% of penicillin-streptomycin (ScienCell, Carlsbad, CA, USA) were grown at 37 °C, 5% CO₂. Primary HHGMCs between passages 2 and 6 were used in all experiments.

Western blotting

Western blot analysis was used to detect pathway proteins,

such as HAPLN1, using antibodies such as anti-T β RI, anti-T β RII (Abcam, Cambridge, UK, 1:2000), anti-GAPDH, anti-MEK1 (Santa Cruz, CA, USA, 1:2000), anti-Raf, anti-p-Raf, anti-ERK1/2, anti-p-ERK1/2, and anti-p-MEK1/2 (Cell Signaling, MA, USA, 1:2000) in cultured HHGMCs. Cells were lysed with RIPA buffer (25 mM, Tris-HCl, 1 mM EDTA, 0.1% Triton-X100) containing complete protease inhibitors (Roche, Mannheim, Germany) and phosphatase inhibitors (Roche, Mannheim, Germany), and the BCA protein assay kit (Pierce Biotechnology, MA, USA) was used for protein quantification. The protein samples were subsequently electrophoresed on 10% and 15% SDS-PAGE gels and transferred onto PVDF membranes. The membranes were blocked with 5% w/v skin milk/ Bovine Serum Albumin (BSA) in TBST (TBS, 0.1% Tween-20) at room temperature for 1 h and incubated with the following primary antibodies overnight. Following washing with TBST, the membranes were incubated with secondary antibody at room temperature for 1 h, washed with TBST and the resulting signals were imaged using ECL reagents (GE Healthcare, UK) as a chemiluminescent substrate. The signals were analyzed and quantified using the computer software Image J (NIH, MD, USA).

Immunoprecipitation

HHGMCs grown on a dish were incubated in ice-cold solution of 0.25 mg/ml EZ-Link™ Sulfo-NHS-LC-Biotin (Thermo Fisher Scientific, MA, USA) at 4 °C for 1 h with gentle shaking on an orbital shaker. Then, 50 mM Tris-HCL (PH 7.5) was added to quench the reaction. The cells were harvested and sonicated with iced-cold lysis buffer (50 mM Tris-HCL, 150 mM NaCl, 1% NP-40, phosphatase inhibitor and protease inhibitor). To remove nonspecific binding, the magnetic beads (protein A beads) and normal rabbit IgG were added and incubated for 1 h at 4 °C. Pre-immobilized anti-biotin antibody-magnetic beads were treated overnight at 4 °C after removal of normal rabbit IgG and magnetic beads. Bound proteins were released by boiling the beads with SDS-sample buffer, subjected to SDS-PAGE, followed by western blotting using the desired antibody.

siRNA and transfection

Small interference RNAs (siRNA) include siHAPLN1 ((Dharmacon; Accell Non-targeting pool, Lafayette, CO, USA), negative control siRNA (Dharmacon; Accell Non-targeting pool, Lafayette, CO, USA), Cluster of Differentiation 44 (CD44) siRNA (Thermo Fisher Scientific; MA, USA), and negative control siRNA (Thermo Fisher Scientific; MA, USA) were used at transfect to HHGMCs using Lipofectamine® RNAiMAX (Thermo Fisher Scientific, MA, USA) in low serum medium for 24 h. The cells were harvested 24 h after transfection.

Cell proliferation assay

A CCK-8 assay was used to determine proliferation according to the manufacturer's protocol. HHGMCs were seeded in 96-well Poly-D-lysine coated plates (Corning® BioCoat™, MA, USA) for 24 h. Then, 10 μ l CCK-8 solution (Enzo Life Sciences, NY, USA) was added to the well and incubated at 37 °C for 1 h. After 1 h of incubation, the absorbance value at 450 nm of each well was measured using a microplate reader, after which the results were statistically analyzed.

Immunofluorescence staining

Immunofluorescence studies were performed using fresh frozen sections having a thickness of 8 μm . The tissue sections were air dried for 1 h and fixed with 4 % paraformaldehyde for 15 min at room temperature. After three washes with phosphate-buffered saline (PBS; Gibco, MA, USA). Nonspecific sites were blocked with PBS with 0.5% normal goat serum at room temperature for 1 h and incubated with primary antibodies overnight at 4 °C in a humidified chamber. The corresponding secondary antibody was conjugated to Alexa Fluor 488 or Alexa Fluor 594 (Invitrogen, MA, USA). Sections were incubated with secondary antibodies for 1 h at room temperature, followed by cell nucleus staining with DAPI for 10 min. Slides mounted with ProLong® Gold antifade reagent with DAPI (Thermo Fisher Scientific, MA, USA) and the staining results were observed microscopically.

Immunohistochemistry staining

Immunohistochemistry staining was performed using the recommended method of the instructions (VECTOR laboratories; VECTASTAIN® ABC kit, CA, USA). Eight micrometer-thick paraffin sections were deparaffinized and incubated in 3% H₂O₂ in the dark. The sections were boiled for 30 min in citrated buffer (10 mM citric acid, 0.05% tween 20, at PH 6.0) for antigen retrieval and cooled for 20 min at room temperature, blocked by 3% BSA in PBS at room temperature for 1 h, and incubated with primary antibodies overnight at 4 °C in a humidified chamber. Sections were incubated with secondary antibodies for 1 h at room temperature, the ABC/DAB solution was added, and the samples were counterstained with hematoxylin. The slides were dehydrated in ethanol and the staining results were observed microscopically.

In-situ hybridization assay

In-situ hybridization (ISH; ACDBio, CA, USA) assay studies were performed using fresh frozen sections with a thickness of 11 μm . The cryosections were fixed in 4% paraformaldehyde at room temperature for 20 min and dehydrated with ethanol. After incubation at room temperature for 10 min with H₂O₂ and incubation at 40 °C for 30 min with a protease. Pre-hybridization and ISH in Hybridize Amp1~6 at 40 °C for 30 min. Respectively, stringent washes with 1X Wash buffers. Equal volumes of BROWN-A and BROWN-B (DAB substrate) were mixed and 120 μl of DAB was pipetted onto each tissue section. The slides were counterstained in 50% Hematoxylin for 2 min for RT and washed for 10 sec in 0.02% ammonia water. Finally, the slides were mounted and the staining results were observed microscopically.

Mice sources and preparation

Pathogen-free, male C57BL/6NCrOri mice (postnatal p23, p27, p32, p37, p40, p44) were purchased from Orient Bio Inc. (Seoul, Korea) and 20-month-old male C57BL/6J mice were purchased from Korea Basic Science Institute (Gwangju, Korea). Animals were quarantined on equal light/dark cycles (12/12 hour) and were food and water *ad libitum* in a controlled environment at 22 \pm 2 °C and with a relative humidity of 50 \pm 5 %. Skin OCT samples were placed into the liquid nitrogen and stored at -80 °C. All procedures and animal treatments were carried out in a clean room of the animal laboratory according to the guidelines for laboratory animal experimentation specified by Chung-Ang University.

Treatment schedule

Progression to the anagen phase was induced by depilation of the skin on the dorsal aspect of mice. Therefore, we shaved the dorsal skin of mice and hair follicles underwent one hair growth cycle for 4–6 weeks. To synchronize the hair growth cycle of mice, this experiment was performed twice. rhHAPLN1 was dissolved in PBS at a concentration of 50 $\mu\text{g}/\text{mL}$ and intraperitoneal injected at a dose of 0.1 mg/kg body weight. The mice were randomized into two groups as follows: (i) the sham group or the vehicle control group received an intraperitoneal injection of PBS; (ii) the rhHAPLN1 group received HAPLN1 at a dose of 0.1 mg/kg body weight. The intraperitoneal injection of rhHAPLN1 was administered every three days for four weeks. The skin sample obtained four weeks after the last haircut. The protocol for animal care and use, observed in this study, was reviewed, and approved by the IACUC at Chung-Ang University (Approval number: 2017-00102).

Statistics

All statistical analyses were performed using the GraphPad Prism 9 software (GraphPad Software, Inc., CA, USA). The data are presented as means \pm standard error of the mean (SEM). Statistical significance was evaluated using a Student's t-test and P-value \leq 0.05 was considered statistically significant (*p < 0.05, **p < 0.001, ***p < 0.0005, and ****p < 0.0001).

Results

HAPLN1 is expressed in hair follicles and promotes the proliferation of HHGMCs through TGF β signaling

After examining HAPLN1 in the skin of young and old mice by immunohistochemistry staining, the results showed that HAPLN1 was located in hair follicles (yellow arrows) and skin fibroblasts (Fig 1A). The level of HAPLN1 and the number of hair follicles were decreased in the skin sections of old mice. The mice hair follicles undergo hair growth cycle twice until postnatal 49 days. The first hair growth cycle is completed in about three and a half weeks (postnatal day 23–25) and the second hair growth cycle begins on postnatal 23 days and ends on postnatal 56 days (Sato, Leopold and Crystal 1999). The time points for the second hair growth cycle are classified into different phases of the hair growth cycle based on established morphological guidelines as follow: early anagen (P23–25), mid anagen (P27), late anagen (P29–34), catagen (P37–39), and telogen (P42). The second telogen lasts more than two weeks, beginning around P42 (Alonso 2006). To confirm how the hair growth stage affected HAPLN1, we used P23, P32, P40, and P44 skin sections (data not shown), and the levels of HAPLN1 were detected by immunofluorescence staining in three stages of the hair growth cycle (Fig 1B). The level of HAPLN1 was significantly increased in the anagen phase, especially in hair bulbs. However, the level of HAPLN1 decreased in the catagen and telogen phases. To investigate HAPLN1 mRNA

level, we compared the three stages of the hair growth cycle (Fig 1C) by morphological criteria using *in-situ* hybridization staining. In the anagen phase, HAPLN1 mRNA was detected in hair bulbs (red arrows). These data show that HAPLN1 may be produced from the hair matrix cells and play an important role in their proliferation, leading to hair growth.

To examine whether HAPLN1 contributes to hair cell proliferation, the HHGMCs were employed and incubated with rhHAPLN1 and/or HA, and the cell viability was analyzed with CCK-8 assay. The results show that the TGF- β 2-dependent proliferation of HHGMCs was significantly promoted in the presence of rhHAPLN1 and/or HA (Fig 1D). Co-localization of HAPLN1 and T β RII was detected in the hair matrix in the anagen phase (Fig 1E). As confirmed in the skin section, HAPLN1 was detected in the hair matrix with a high rate of cell proliferation, suggesting that HAPLN1 may be an essential factor for cell proliferation.

rhHAPLN1 selectively enhanced the level of T β RII in HHGMCs

We examined the effect of rhHAPLN1 on the levels of TGF- β receptor I and II in HHGMCs using western blotting. rhHAPLN1 increased the level of T β RII at a concentration of 20 ng/mL (Fig 2A), and significantly increased the T β RII levels when combined with HA (Fig 2B). This suggests that such increases by rhHAPLN1 and/or HA may be due to the formation of a huge PGs-rhHAPLN1-HA-CD44-T β RII complex, as previously described (Bourguignon et al. 2002; Harada and Takahashi 2007), thereby preventing the rate of endocytic degradation of the T β RII.

To examine whether T β RII levels are down-regulated by the knock-down of HAPLN1, HHGMCs were transfected with either negative control siRNA or siRNA against HAPLN1 (siHAPLN1). The siHAPLN1 reduced endogenous HAPLN1 and concurrent reduction of the T β RII levels (Fig 2C). When siHAPLN1-transfected HHGMCs were treated with rhHAPLN1 and/or HA, the T β RII levels were significantly restored (Fig 2D). Thus, we suggest that endogenous HAPLN1 may play an important role in enhancing or maintaining the T β RII level. On the other hand, to investigate whether rhHAPLN1 depends on HA to increase the T β RII levels, 4-methylumbelliferone (4-MU), an inhibitor of hyaluronan synthase 2 (HAS2), was employed (Kultti et al. 2009). 4-MU significantly decreased T β RII and HAS2 expression levels, but rhHAPLN1 restored T β RII and HAS2 expression levels (Fig 2E), suggesting that HA may restore the reduced T β RII level through rhHAPLN1.

CD44 is essential for rhHAPLN1 to increase the level of T β RII

It is well known that HA binds to the CD44 receptors, and these complexes seem to be further associated with T β RII at the cell surface, leading to activation of TGF- β signaling (Bourguignon et al. 2002). To evaluate the effect of CD44 knockdown on HAPLN1-regulated T β RII, cells were transfected with negative control and CD44 siRNA. Our results showed that the knockdown of CD44 inhibited T β RII level (Fig 3A). Moreover, following treatment with HA and/or rhHAPLN1 on CD44 siRNA-transfected HHGMCs, T β RII levels were not restored by HA and/or rhHAPLN1 (Fig 3B). The results indicate that CD44 is an essential factor in the action of rhHAPLN1 on the regulation of T β RII level.

rhHAPLN1 and HA increase the level of cell surface membrane T β RII by the treatment of TGF- β 2 in HHGMCs

Previous findings suggested that HA and HAPLN1 exert their effects at the level of the cell membrane. This is because extracellular HA and HAPLN1 were found to regulate T β RII, and CD44 was found to play a crucial role in this process. In treatment with HA and/or rhHAPLN1 on HHGMCs, cell surface proteins were labeled with sulfo-NHS-LC-biotin and then separated using immunoprecipitation analysis. As per the results, the exogenous HA and rhHAPLN1 increased the level of T β RII at the cell surface membrane in HHGMCs (Fig 4). These results imply that the increased levels of T β RII by rhHAPLN1 and/or HA may indeed be through a mechanism at the cell membrane.

rhHAPLN1 and HA promote TGF- β 2 signaling through the ERK1/2-mediated non-canonical pathway

It has been previously shown that the heteromeric receptor complexes between T β RI and T β RII mediated by TGF- β stimulate distinct downstream signaling pathways, Smad-dependent and Smad-independent pathways, also termed canonical and non-canonical pathways, respectively, to regulate different context-dependent transcription factors (Massague, Blain and Lo 2000). That is, the canonical TGF- β signaling pathway uses Smad2 and/or Smad3 to transfer signals. Smad2/3 are directly phosphorylated by T β RI and translocate to the nucleus to regulate gene transcription (Massague, Blain and Lo 2000). One of the non-canonical TGF- β signaling pathways involves ERK/MAPK kinase. The ERK/MAPK pathway is induced by various stimuli. Thus, we investigated whether the TGF- β 2 signaling occurred through the Smad-dependent or Smad-independent pathway. No changes in phosphorylation of Smad2 was observed by the treatment of rhHAPLN1 and/or HA (Fig 5A). In contrast, interestingly, p-ERK1/2, p-MEK1/2, and p-c-Raf, which are known as the effectors activated downstream of the Smad-independent pathway, were significantly increased in the presence of rhHAPLN1 and/or HA (Fig 5B). These results highlight that the TGF- β 2 signaling could undergo via the non-canonical ERK1/2 pathway.

HAPLN1 stimulates hair growth in mice

Our previous results indicating the loss of HAPLN1 in the aging process, prompted us to adapt old mice for an *in vivo* experiment. Each of the mice has been shown to enter the different hair growth cycles after the second hair growth cycle. To synchronize the hair growth cycle, the old mice were clipped, and depilatory cream was applied to stimulate the whole skin. In old mice, hair follicles enter the anagen phase earlier in the HAPLN1 treatment group compared to the vehicle group (Fig 6).

Discussion

Hair loss in a part of the head has been known to be due to various causes, such as drugs, stresses, and autoimmune disorders. Various therapeutic agents have been shown

depending on the cause of the condition, as well as patient sex and age (Kim et al. 2022). This study is the first to describe the newly discovered effects of full-length rhHAPLN1 on hair growth of old mice as well as the underlying mechanisms in HHGMCs. Indeed, HAPLN1 has been shown to bind noncovalently to a specific region of proteoglycan protein and a filament of HA and stabilizes the reversible noncovalent binding between. Thus, HA-PGs complexes known as ‘aggregates’ are formed in the PCM (Hardingham 1979; Buckwalter et al. 1984; C B Knudson 1993). It has long been known that the aggregate formed in the presence of HAPLN1, termed ‘HAPLN1-containing aggregate’ is five times longer and has three times more proteoglycans compared to HAPLN1-free aggregate because the former leads to an increased stability of the linking between proteoglycans and HA (et al. 1984). Thus, HAPLN1 can largely contribute to the formation of a water-rich and viscoelastic hydrogel matrix (Warren et al. 2021).

A previous study showed that the exogenous HA induced the trafficking of T β R to caveolin-1 lipid raft-associated pools and caused T β R degradation (Ito et al. 2004). Of note, the present study demonstrates that the treatment with rhHAPLN1 and/or HA selectively increased the levels of T β RII, not T β RI, at the cell surface membrane in HHGMC. Although at present, the precise mechanisms by which rhHAPLN1 increased the levels of T β RII, rhHAPLN1 seems to inhibit the internalization of T β RII by preventing the degradation of HA (Govindan and Iovine 2014). In this context, it should be noted that the degradation of HA is essential for the endocytosis of large HA molecules (Hua et al. 1993; Danielson et al. 2015), and this process involves CD44, the main receptor of HA (Harada and Takahashi 2007). Since T β Rs is known to be directly linked to CD44, and the degradation of HA is required for the endocytosis of T β R (Bourguignon et al. 2002; Ito et al. 2004). Additionally, as aforementioned, the HAPLN1-containing aggregate binds to CD44 as a bulky and water-rich hydrogel ligand, forming a huge size of complex consisted of the aggregate-CD44-T β Rs, and thereby slowing down the rate of endocytic degradation of T β RII. Therefore, our data suggest that rhHAPLN1 could contribute to the increase in the levels of T β RII by preventing the degradation of HA, enabling the aggregate-containing complexes to remain functional on the membrane. Moreover, our results indicate that exogenous HA and/or rhHAPLN1 increase the level of cell surface membrane T β RII in the presence of TGF- β 2, suggesting that rhHAPLN1 and/or HA may decrease the internalization rate of T β RII, and subsequently enhance the TGF- β 2-signaling through such an increase in the number of T β RII on the cell surface membrane. Our results show that when membrane proteins are labeled with sulfo-NHS-LC-biotin, the increased levels of T β RII were shown in HA- and/or rhHAPLN1-treated HHGMCs through an immunoprecipitation analysis, further indicating the decreased rate of the endocytic degradation of T β RII.

Importantly, we found that both the HA and CD44 are likely to be essential for rhHAPLN1 to act on HHGMCs and regulate TGF- β 2 signaling. When production of endogenous HA was inhibited by the HAS2 inhibitor 4-MU, the levels of T β RII were significantly decreased, suggesting an important role of HA as a molecule connecting between T β RII and rhHAPLN1. Furthermore, in CD44-knockdown HHGMCs, T β RII was not only decreased compared with the control, but also unaffected by the treatment of HA and/or

rhHAPLN1, highlighting the important roles of CD44 in the enhancement of T β RII by rhHAPLN1. Unlike young mice, old mice have been shown to exhibit different hair growth cycles for each individual (Plikus and Chuong 2008). In this regard, old mice were clipped and depilatory cream was applied to stimulate the whole skin. The hair growth cycle was promoted by skin stimulation and the above procedure was repeated twice to synchronize the hair growth cycle of all old mice. After the second hair growth cycle, we clipped hair coats in the telogen phase and treated them with rhHAPLN1. Compared with the vehicle-treated group, the group that received intraperitoneal injections of rhHAPLN1 showed that the hair follicles entered the hair growth phase (anagen) earlier. rhHAPLN1 seems to play a role in optimizing an environment for cell proliferation and differentiation, allowing hair follicles to enter the anagen phase *in vivo*.

Taken together, the present study findings show that the treatment of rhHAPLN1 and/or HA can result in an increase in T β RII protein levels, thus leading to the enhancement of TGF- β 2-ERK1/2 signaling via non-canonical TGF- β signaling pathways. In addition, these data imply that T β RII may be subjected to its degradation via an endocytic process, but this degradation pathway may be slowed down or inhibited by the mechanochemical properties of rhHAPLN1. Interestingly, the intraperitoneal injections of rhHAPLN1 into old mice showed that the hair follicles entered the hair growth phase (anagen) earlier, allowing hair follicles to enter the anagen phase *in vivo*. Thus, rhHAPLN1 may act as a novel biomechanical signaling protein promoting hair growth.

Conflicts of Interest

D. Zhou, Z. Fu, JM. Jang, and IC. Shin are employees of HaplnScience Inc. JM. Jang and DK. Kim are shareholders of HaplnScience Inc.

Acknowledgments

This study was supported by a Chung-Ang University Young Scientist Scholarship in 2015, and also supported by a grant from the National Research Foundation of Korea (NRF-2017M3A9D8048414) funded by the Korean government (Ministry of Science and ICT).

References

- Alonso L (2006) The hair cycle. *J Cell Sci* 119:391-393.
- Binette F, Cravens J, Kahoussi B, Haudenschield DR, Goetinck PF (1994) Link protein is ubiquitously expressed in non-cartilaginous tissues where it enhances and stabilizes the interaction of proteoglycans with hyaluronic acid. *J Biol Chem* 269:19116-19122.
- Bourguignon LY, Singleton PA, Zhu H, Zhou B (2002) Hyaluronan promotes signaling interaction between CD44 and the transforming growth factor beta receptor I in metastatic breast tumor cells. *J Biol Chem* 277: 39703-12.
- Buckwalter JA, Rosenberg LC, Tang LH (1984) The effect of link protein on proteoglycan aggregate

- structure. An electron microscopic study of the molecular architecture and dimensions of proteoglycan aggregates reassembled from the proteoglycan monomers and link proteins of bovine fetal epiphyseal cartilage. *J Biol Chem* 259:5361-5363.
- Chase HB (1954) Growth of the hair. *Physiol Rev* 34:113-126.
- Campiche R, Jackson E, Laurent G, Roche M, Gougeon S, Sérroul P, Ströbel S, Massironi M, Gempeler M (2019) Skin Filling and Firming Activity of a Hyaluronic Acid Inducing Synthetic Tripeptide. *Int J Pept Res Ther* 26:181-189.
- Derynck R, Zhang YE (2003) Smad-dependent and Smad-independent pathways in TGF-beta family signaling. *Nature* 425:577-584.
- Danielson BT, Knudson CB, Knudson W (2015) Extracellular processing of the cartilage proteoglycan aggregate and its effect on CD44-mediated internalization of hyaluronan. *J Biol Chem* 290:9555-9570.
- Foitzik K, Lindner G, Mueller-Roever S, Maurer M, Botchkareva N, Botchkarev V, Handjiski B, Metz M, Hibino T, Soma T, Dotto GP, Paus R (2000) Control of murine hair follicle regression (catagen) by TGF-beta1 in vivo. *FASEB J* 5:752-760.
- Foitzik K, Paus R, Doetschman T, Dotto GP (1999) The TGF-beta2 isoform is both a required and sufficient inducer of murine hair follicle morphogenesis. *Dev Biol* 212:278-289.
- Govindan J, Iovine MK (2014) Hapln1a is required for connexin43-dependent growth and patterning in the regenerating fin skeleton. *PLoS One*, 9:e88574.
- Hibino T, Nishiyama T (2004) Role of TGF-beta2 in the human hair cycle. *J Dermatol Sci* 35:9-18.
- Huang F, Chen YG (2012) Regulation of TGF-beta receptor activity. *Cell Biosci* 2: 9.
- Hardingham TE (1979) The role of link-protein in the structure of cartilage proteoglycan aggregates. *Biochem J* 177:237-247.
- Harada H, Takahashi M (2007) CD44-dependent intracellular and extracellular catabolism of hyaluronic acid by hyaluronidase-1 and -2. *J Biol Chem* 282: 5597-5607.
- Hua Q, Knudson CB, Knudson W (1993) Internalization of hyaluronan by chondrocytes occurs via receptor-mediated endocytosis. *J Cell Sci* 106 (Pt 1): 365-375.
- Ito T, Williams JD, Fraser DJ, Phillips AO (2004) Hyaluronan regulates transforming growth factor-beta1 receptor compartmentalization. *J Biol Chem* 279:25326-25332.
- Kim MJ, Seong KY, Kim DS, Jeong JS, Kim SY, Lee S, Yang SY (2022) An BS. Minoxidil-loaded hyaluronic acid dissolving microneedles to alleviate hair loss in an alopecia animal model. *Acta Biomater* 143:189-202.
- Kultti A, Pasonen-Seppanen S, Jauhiainen M, Rilla KJ, Karna R, Pyoria, Tammi RH & M. I. Tammi (2009) 4-Methylumbelliferone inhibits hyaluronan synthesis by depletion of cellular UDP-glucuronic acid and downregulation of hyaluronan synthase 2 and 3. *Exp Cell Res* 315:1914-1923.
- Knudson CB, Knudson WK (1993) Hyaluronan-binding proteins in development, tissue homeostasis, and disease. *FASEB J* 7(13):1233-1241.
- Mori O, Hachisuka H, Sasai Y (1996) Effects of transforming growth factor beta 1 in the hair cycle. *J Dermatol* 23:89-94.
- Massague J, Blain SW, Lo RS (2000) TGFbeta signaling in growth control, cancer, and heritable disorders. *Cell* 103:295-309.
- Niimori D, Kawano R, Felemban A, Niimori-Kita K, Tanaka H, Ihn H, Ohta K (2012) Tsukushi controls the hair cycle by regulating TGF-beta1 signaling. *Dev Biol* 372(1):81-87.
- Neuzillet C, Hammel P, Tijeras-Raballand A, Couvelard A, Raymond E (2013) Targeting the Ras-ERK pathway in pancreatic adenocarcinoma. *Cancer Metastasis Rev* 32:147-162.
- Oshimori N, Fuchs E (2012) Paracrine TGF-beta signaling counterbalances BMP-mediated repression in hair follicle stem cell activation. *Cell Stem Cell* 10:63-75.
- Philpott MP, Green MR, Kealey T (1990) Human hair growth in vitro. *J Dermatol Sci* 97(p3):463-471.
- Papakonstantinou E, Roth M, Karakiulakis G (2012) Hyaluronic acid: A key molecule in skin aging. *Dermatol Endocrinol* 4:253-258.
- Plikus MV, Chuong CM (2008) Complex Hair Cycle Domain Patterns and Regenerative Hair Waves in Living Rodents. *J Investigative Dermatol* 128: 1071-1080.
- Spicer AP, Joo A, Bowling RA (2003) A hyaluronan binding link protein gene family whose members are physically linked adjacent to chondroitin sulfate proteoglycan core protein genes: the missing links. *J Biol Chem* 278:21083-21091.
- Sato N, Leopold PL, Crystal RG (1999) Induction of the hair growth phase in postnatal mice by localized transient expression of Sonic hedgehog. *J Clin Invest* 104:855-864.
- Taghiabadi E, Nilforoushadeh MA, Aghdami N (2020) Maintaining Hair Inductivity in Human Dermal Papilla Cells: A Review of Effective Methods. *Skin Pharmacol Physiol* 33:280-292.
- Tang P, Wang X, Zhang M, Huang S, Lin C, Yan F, Deng Y, Zhang L, Zhang L (2019) Activin B Stimulates Mouse Vibrissae Growth and Regulates Cell Proliferation and Cell Cycle Progression of Hair

Matrix Cells through ERK Signaling. *Int J Mol Sci* 20(4):853.

Warren JP, Miles DE, Kapur N, Wilcox RK, Beales PA (2021) Hydrodynamic Mixing Tunes the Stiffness of Proteoglycan-Mimicking Physical Hydrogels. *Adv Healthc Mater* 10:e2001998.

Xi J, Ting YL, Xue L, Dan L (2021) Effect of hyaluronic acid: Mechanistic investigations via topological and functional analysis of its protein interaction network. *Tropical J Pharmaceut Res* 18:1919-1925.

Figure legends:

Figure 1. Expression of HAPLN1 indifferent stages of hair growth cycle and HAPLN1 enhanced the proliferation of HHGMCs

(A) Immunohistochemical staining of frozen sections of skin tissue. HAPLN1 (yellow arrows) staining of biopsies taken from 7-week-old mice and 20-month-old mice kept in conventional conditions. Original magnifications: 100 X and 200 X. (B) Localization and characterization of HAPLN1 in the hair follicles of mice during each phase of the hair cycle. Localization of HAPLN1 in the hair follicles during telogen, anagen and catagen phases. The levels of HAPLN1 were significantly increased in the anagen phase. Original magnifications: 400 X. (C) In situ hybridization detection of HAPLN1 mRNA in each stage of hair growth cycle. HAPLN1 mRNA was detected in hair bulbs in the anagen phase. The tissue sections were stained with HAPLN1 RNA probe according to the standard procedures (original magnification, 400 X). (D) HHGMCs were pretreated with HAPLN (25 ng/ml) and/or HA (25 µg/ml) for 1 h prior to stimulation with TGF-β2 (2 ng/ml) for 23 h. The cell proliferation was analyzed with the CCK-8 assay. The results (the mean ± S.E.M.) are representative of four independent experiments (n=4). * p < 0.05. (E) Immunofluorescence staining of frozen sections of skin tissue. Localization of HAPLN1 in the hair growth cycle during telogen, anagen, and catagen phases. Co-localization of HAPLN1 and TβRII were detected in the anagen phase (original magnification, 400 X).

Figure 2. HAPLN1 and/or HA increased TβRII levels expression in HHGMCs

(A) The plot and relative quantification of the expression of TβRII in HHGMCs treated with various doses (0 ng/ml; 5 ng/ml; 10 ng/ml; 20 ng/ml) HAPLN1 for 24 h. (B) The plot and the relative quantification of the expression of TβRII in cells pretreated with HAPLN1 (25 ng/ml) and/or HA (25 µg/ml) for 1 h prior to stimulation with TGF-β2 (2 ng/ml) for 23 h. (C) The plot and the relative quantification of the expression of TβRII in HHGMCs following HAPLN1 knockdown. (D) The plot and relative quantification of the expression of TβRII in HAPLN1 knockdown HHGMCs pretreated with HAPLN1 (25 ng/ml) and/or HA (25 µg/ml) for 1 h prior to stimulation with TGF-β2 (2 ng/ml) for 23 h. (E) The plot and the relative quantification of the expression of TβRII and HAS2 in HHGMCs pretreated with 4-MU (0.5

mM) and/or HAPLN1 (25 ng/ml) for 1 h prior to stimulation with TGF-β2 (2 ng/ml) for 23 h. The results (the mean ± S.E.M.) are representative of three independent experiments (n=3). * p < 0.05, ** p < 0.01, *** p < 0.001.

Figure 3. Lack of endogenous CD44 decreased TβRII levels expression in hair matrix cells

(A) The plot and the relative quantification of the expression of TβRII in CD44 following HAPLN1 knockdown. (B) The plot and the relative quantification of the expression of TβRII in CD44 knockdown HHGMCs pretreated with HAPLN1 (25 ng/ml) and/or HA (25 µg/ml) for 1 h prior to stimulation with TGF-β2 (2 ng/ml) for 23 h. The results (the mean ± S.E.M.) are representative of three independent experiments (n=3). * p < 0.05, ** p < 0.01, *** p < 0.001.

Figure 4. HAPLN1 and/or HA increased TβRII levels expression in hair matrix cells surface membrane.

The plot and the relative quantification of the expression of TβRII in cells pretreated with HAPLN1 (25 ng/ml) and/or HA (25 µg/ml) for 1 h prior to stimulation with TGF-β2 (2 ng/ml) for 23 h. Cell surface levels of TβRII were defined by labeling cells with sulpho-NHS-LC-biotin. Immunoprecipitation study was performed using an antibody against biotin. The results (the mean ± S.E.M.) are representative of three independent experiments (n=3). * p < 0.05, ** p < 0.01, *** p < 0.001.

Figure 5. HAPLN1 and/or HA activate non-canonical pathway of TGF-β2-ERK1/2 signaling.

The plot and the relative quantification of the expression of phosphorylation of (A) Smad2, (B) c-Raf, ERK1/2 and MEK1/2 in cells pretreated with HAPLN1 (25 ng/ml) and/or HA (25 µg/ml) for 1 h prior to stimulation with TGF-β2 (2 ng/ml) for 23 h. The results (the mean ± S.E.M.) are representative of four independent experiments (n=4). * p < 0.05, ** p < 0.01, *** p < 0.001.

Figure 6. HAPLN1 promotes hair regrowth in mice.

20 month-old male C57BL/6 mice were depilated and were treated with HAPLN1, beginning the day after hair removal, three times per week. Photographs were taken on days 0, 8, and 21 days after depilation. From 8 days, HAPLN1 groups showed notable darkening of skin color, and over time they showed a markedly greater hair growth than the PBS group.

Figures

Figure 1

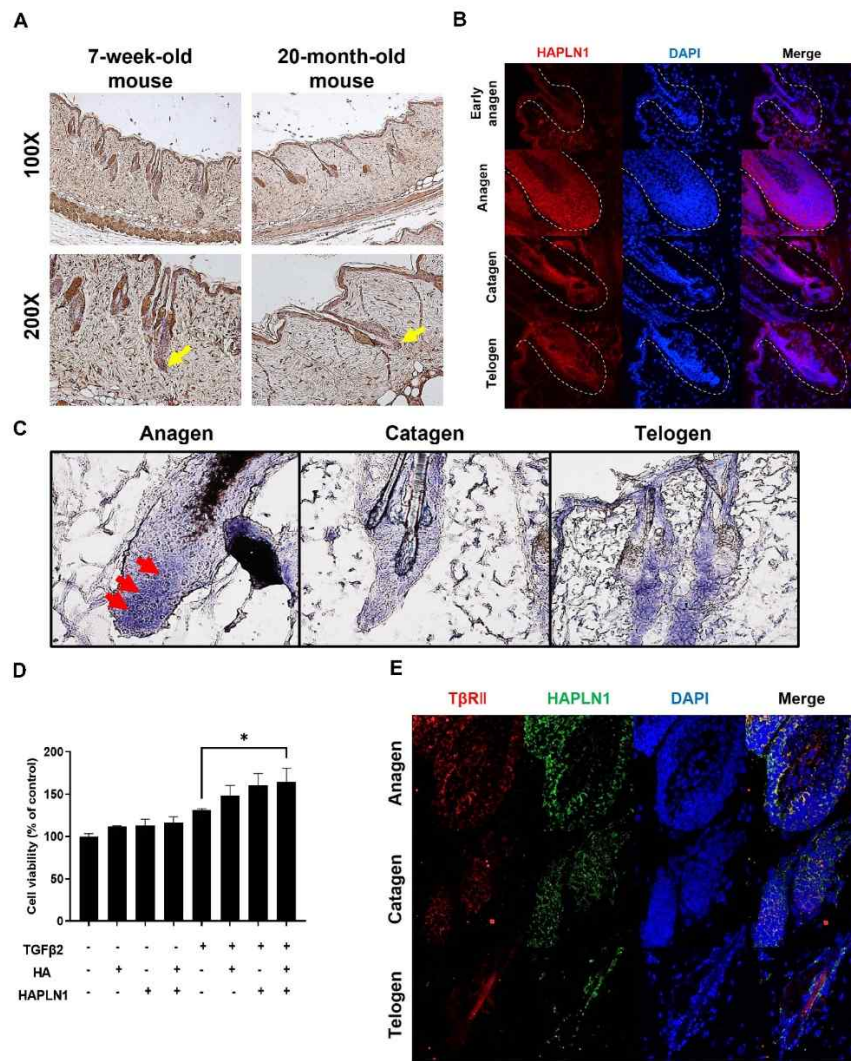


Figure 2

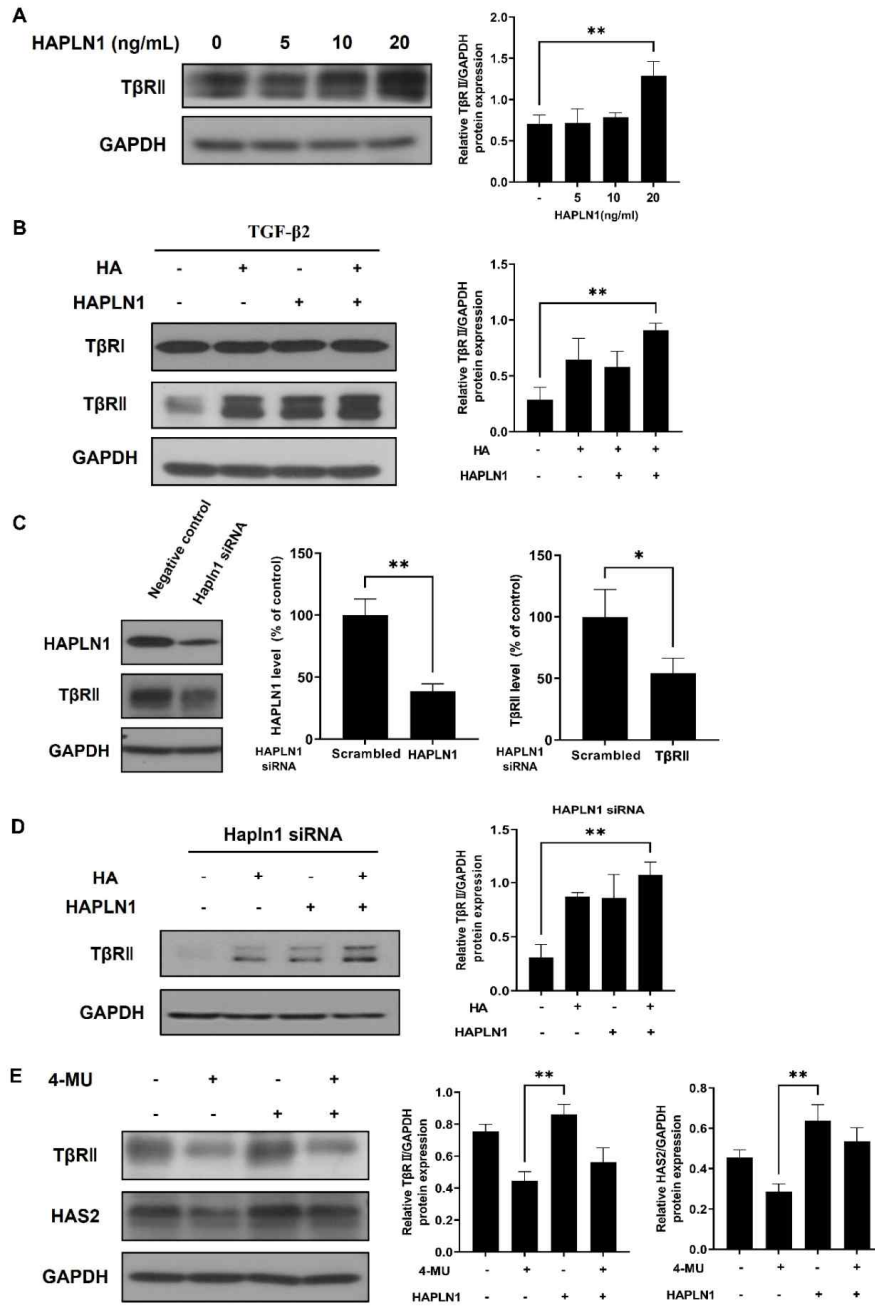


Figure 3

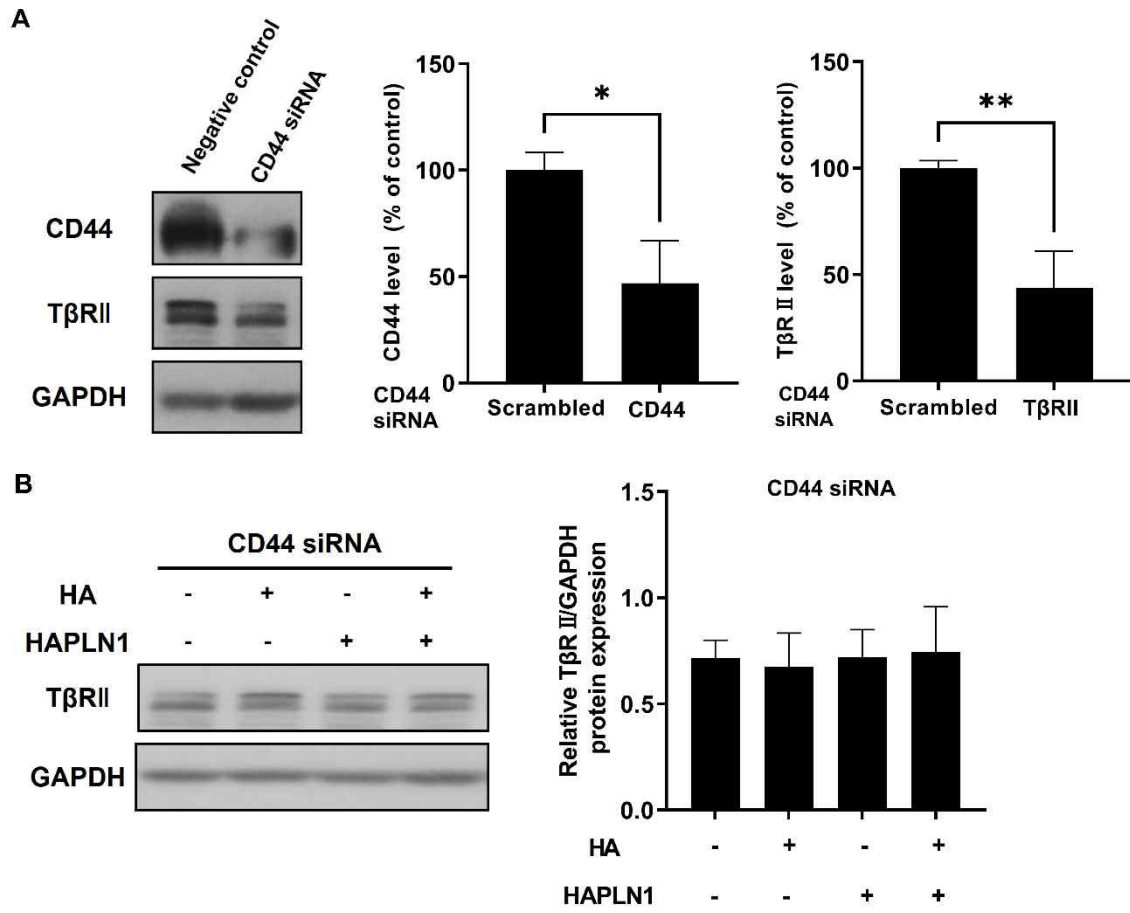


Figure 4

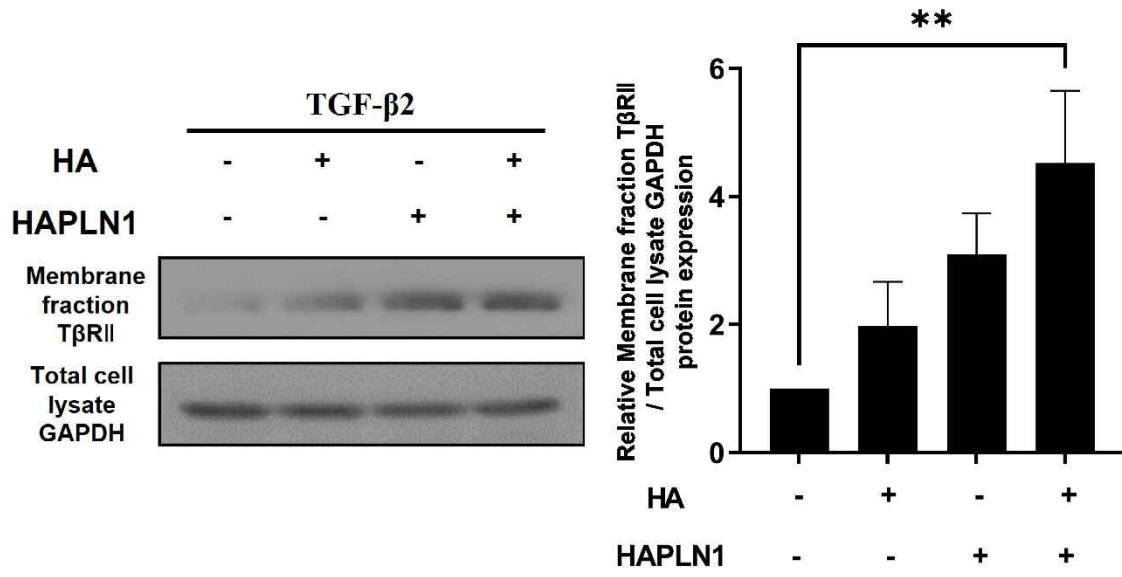
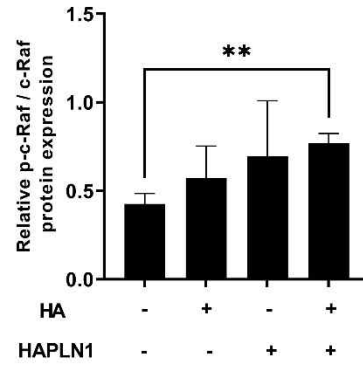
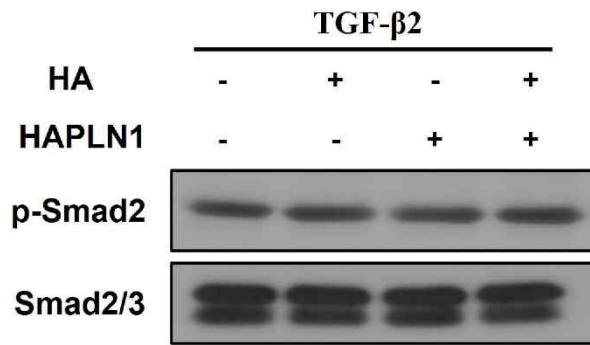


Figure 5

A



B

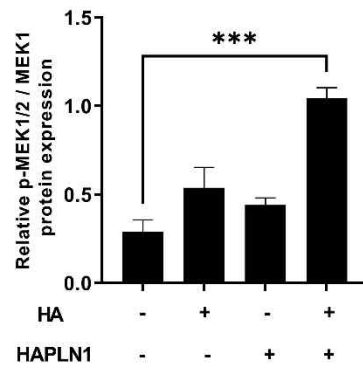
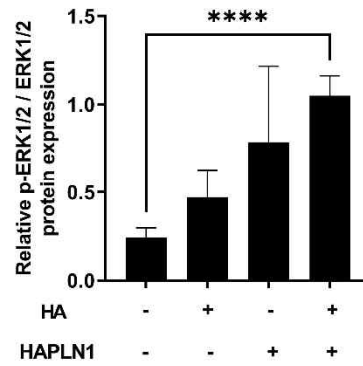
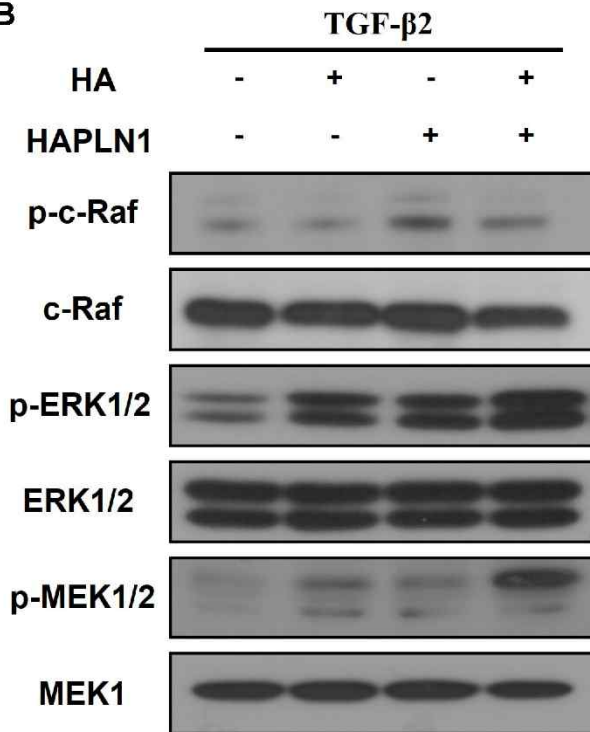


Figure 6

